

Chicago Spectral Distortion Workshop

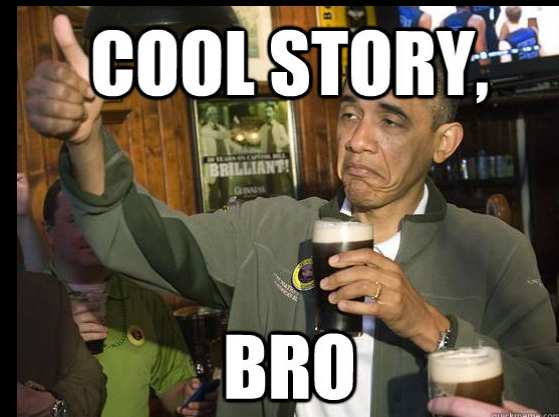
# What do we learn from Spectral Distortions? Theory for Experimentalists

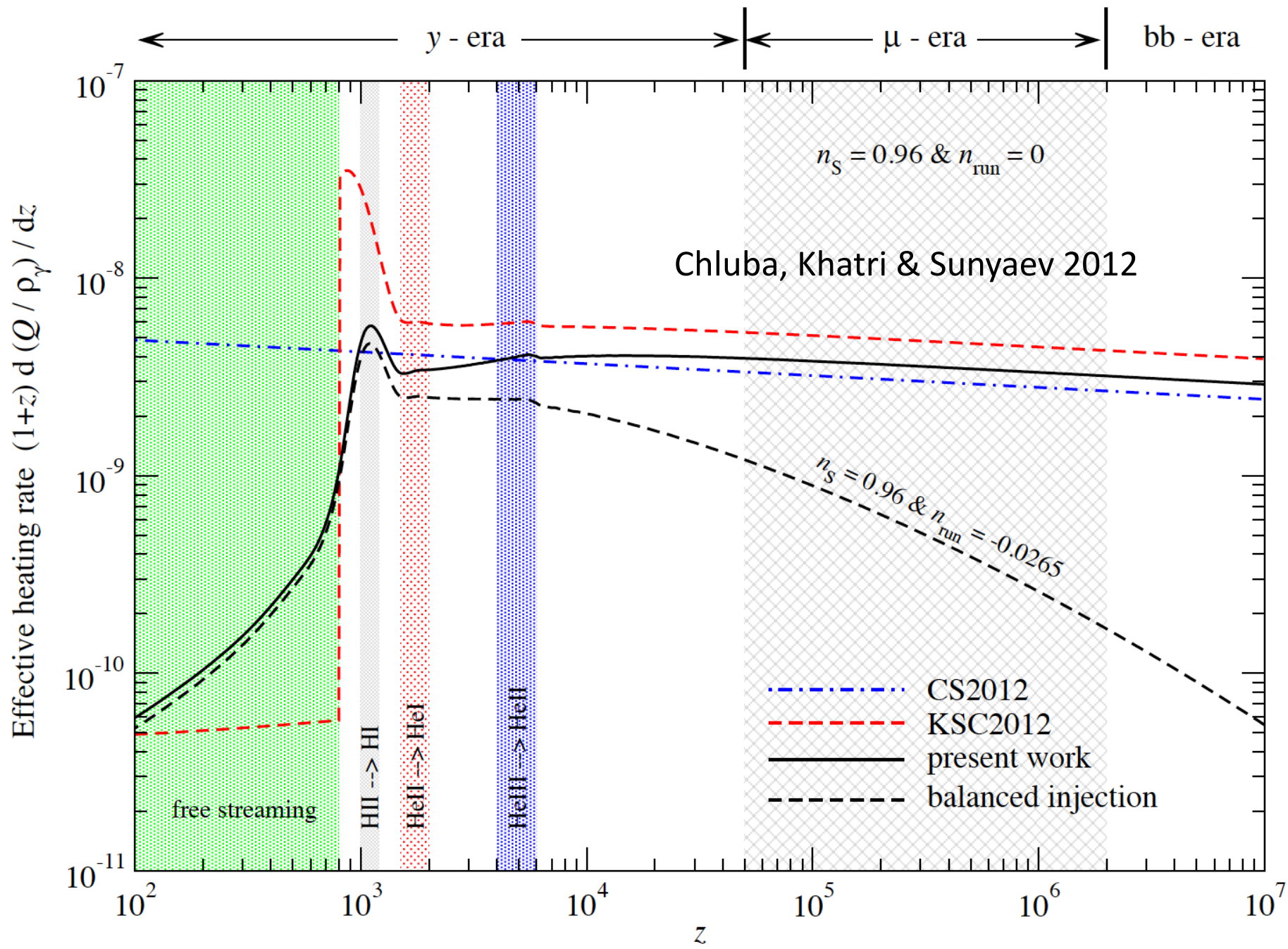
David Spergel

Princeton

# Thermal History of Universe

- Energy injection at  $z \gg 10^6$  changes temperature-time relation
- During  $4 \times 10^4 < z < 2 \times 10^6$  energy injection produces  $+\mu$  distortions (adiabatic cooling produce  $-\mu$  distortions)
- Energy injection after recombination produces  $y$  distortions





# Energy Injection in the first month

- $z \gg 2 \times 10^6$ , double Compton and Bremsstrahlung interactions of photons with electron-ion plasma was very efficient.
- Changes temperature-time relation

# Energy injection in the $\mu$ era

- Adiabatic cooling produce a negative  $\mu$  distortion  $\mu = -2.2 \times 10^{-9}$  (Chluba and Sunyaev 2012)
  - NR matter redshifts as  $(1+z)^2$
  - Electrons “cool” CMB
- Damping of acoustic waves heats the universe and produce a positive  $\mu$  distortion

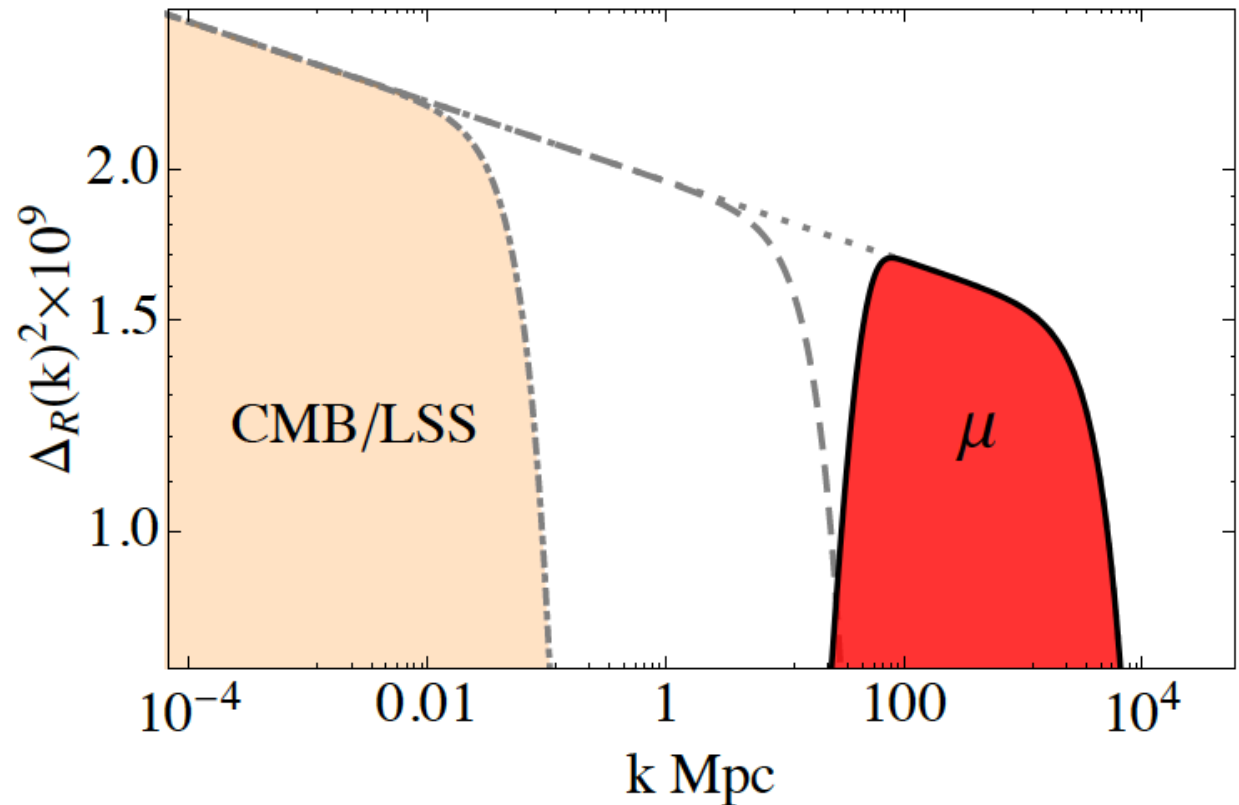
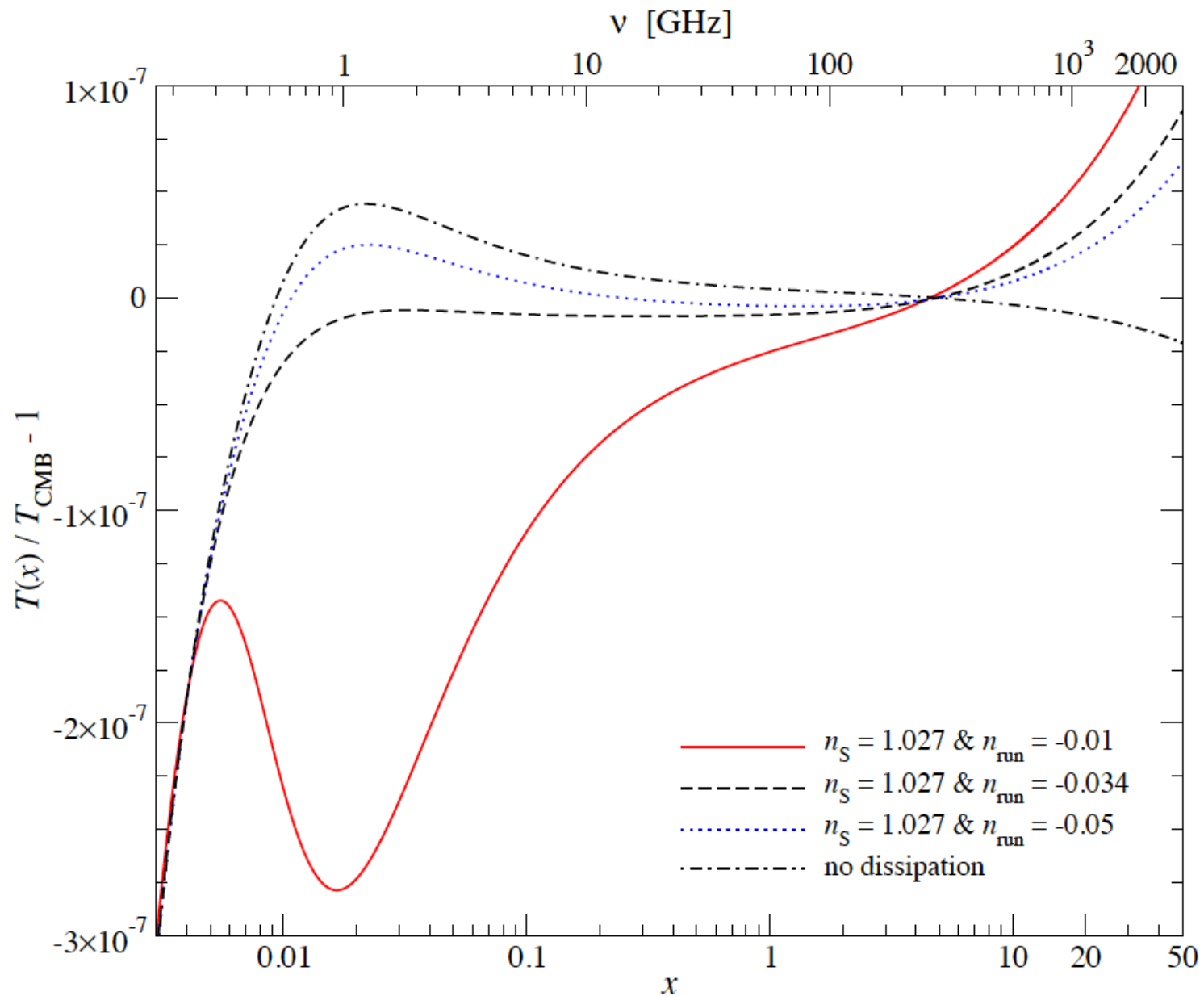
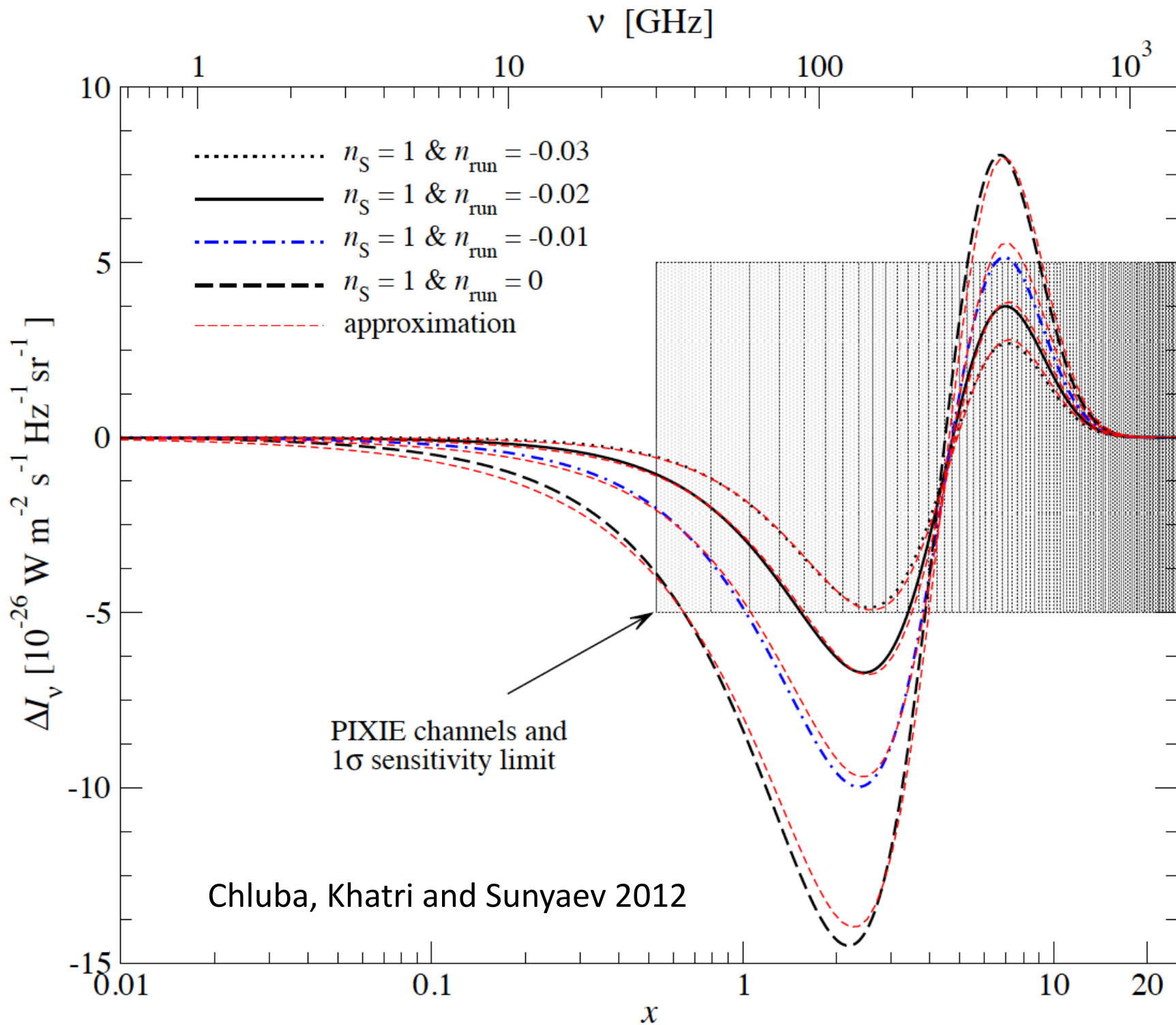


Figure 1: The figure shows the power spectrum with Silk damping as function of  $\log k$ . The dotted, dashed and dot-dashed lines are  $\Delta_R^2 e^{-2k^2/k_D^2}$  at  $z_{\mu,i} = 2 \times 10^6$ ,  $z_{\mu,f} = 5 \times 10^4$  and  $z_L = 1100$  respectively. The red area on the right indicated by  $\mu$  is the difference of the power spectrum between  $z_{\mu,i}$  and  $z_{\mu,f}$ . Once integrated over  $\log k$  this gives the  $\mu$ -distortion. For comparison on the left we have highlighted the scales probed by LSS and CMB anisotropies.



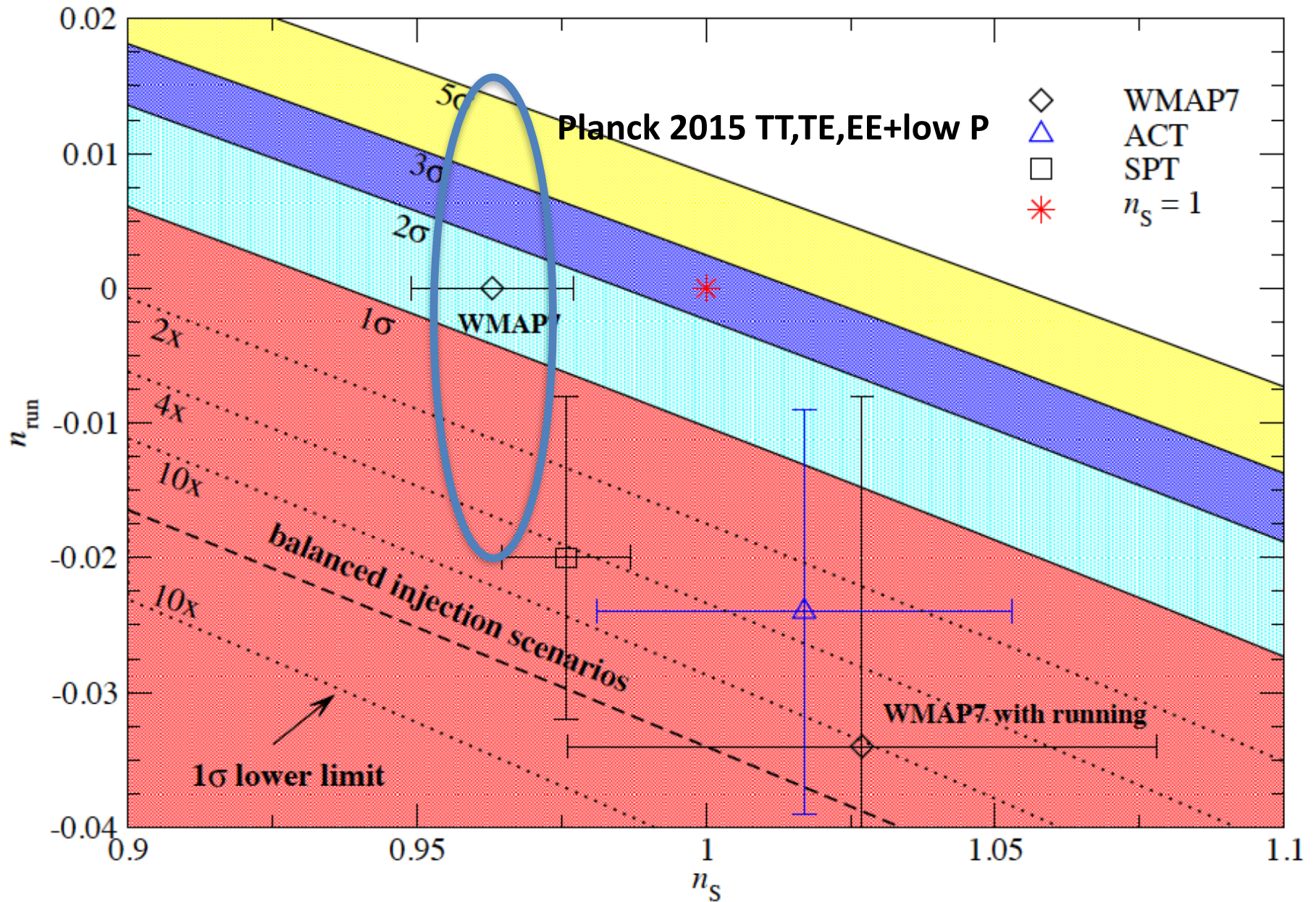
**Figure 11.** Spectral distortion from acoustic damping and BE condensation for  $n_s = 1.027$  and  $n_{\text{run}} = -0.01, -0.034, -0.05$ . The balanced scenario is very close to  $n_{\text{run}} = -0.034$ . For comparison we also show the case without any dissipation.





possible constraints from  $\mu$

CKS 2012



# Non-Gaussianities and $\mu$ distortions

- Potential ability to probe very small values of  $f_{NL}$
- Harder to see than  $\mu$  distortions.  
Detection requires large NG signal on small scales

$$\frac{S}{N} \simeq 0.7 \times 10^{-3} b f_{NL} \left( \frac{\sqrt{4\pi} \times 10^{-8}}{w_{\mu}^{-1/2}} \right).$$

Pajer and Zaldarriaga 2012

# Y distortions: Groups Win!

- Small scale CMB fluctuations ( $8 \times 10^{-10}$  [Chluba and Sunyaev 2004])
- Acoustic waves  $4 \times 10^{-9}$  (CKS 2012)
- Reionization  $10^{-7}$  (Hill et al. 2015)
- IGM  $10^{-7}$
- **Clusters + Groups  $10^{-6}$**  (KS 2015:  $> 5.4 \times 10^{-8}$ )

$$\left\langle \tau_e \frac{kT_e}{m_e c^2} \right\rangle$$

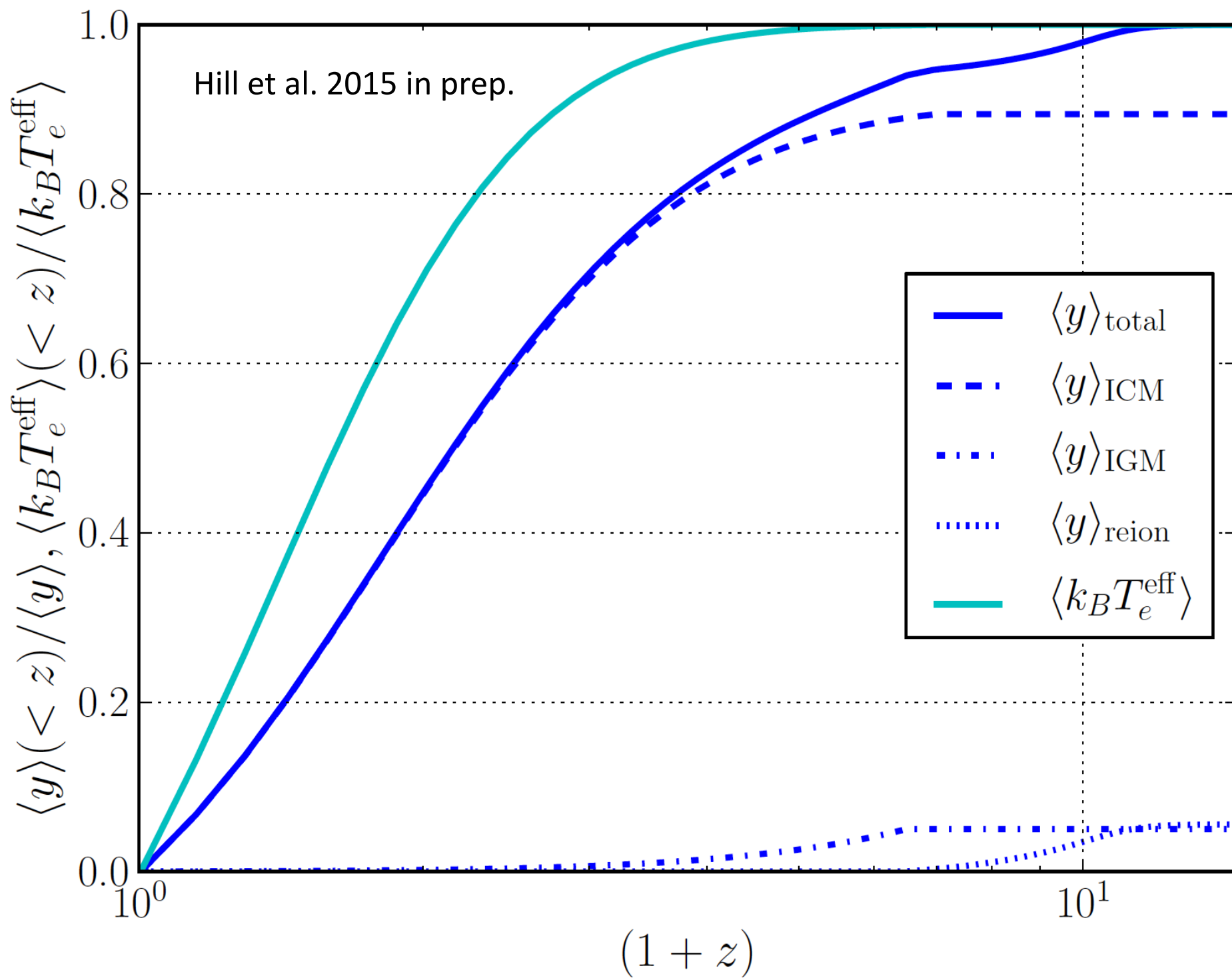
Hill et al. 2015

$$1.6 \times 10^{-6} \left( \frac{\sigma_8}{0.80} \right)^5$$

# Group and Clusters

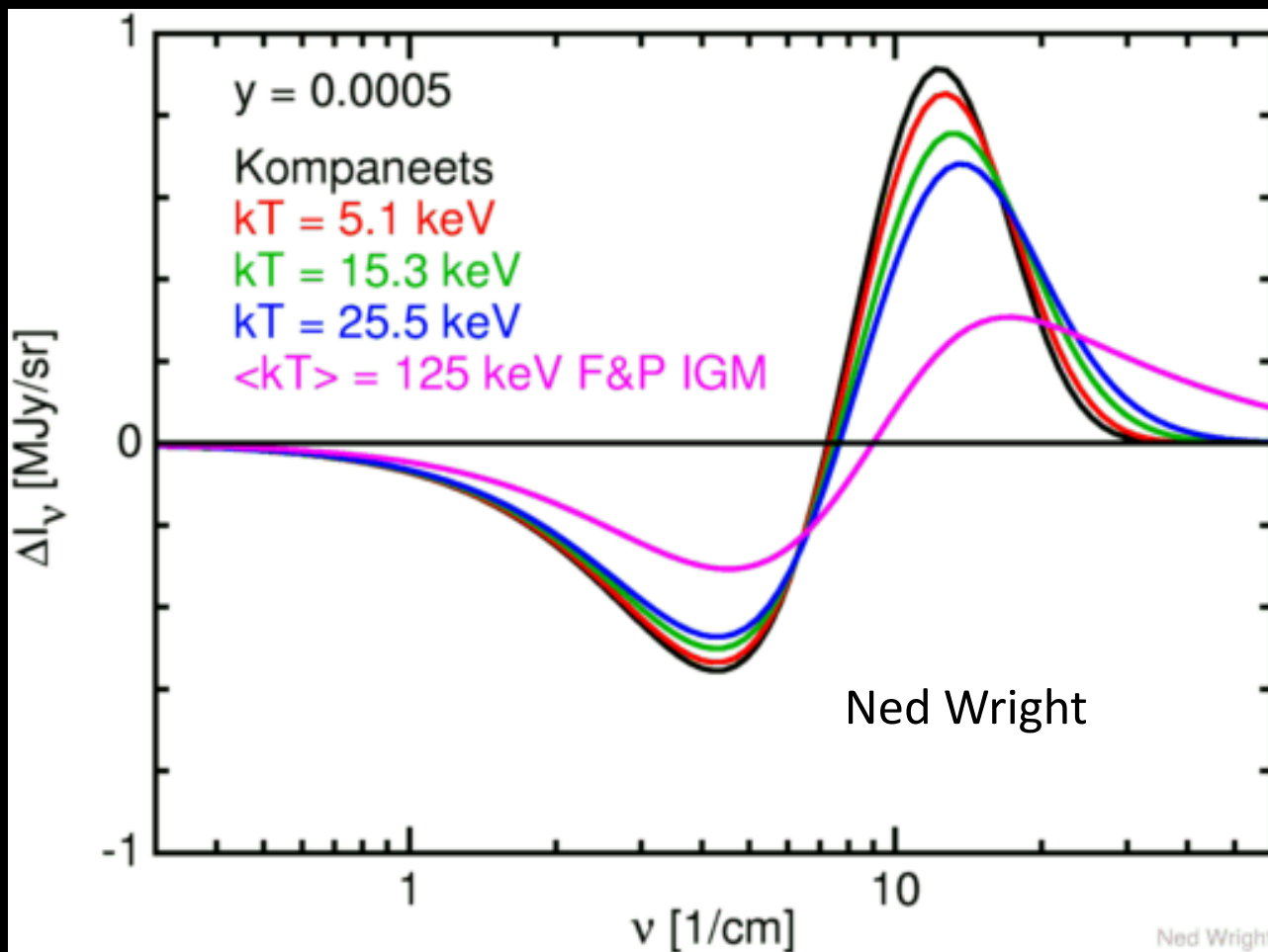
- From  $10^{13}$  -  $10^{14}$  solar mass clusters at  $z \sim 1$
- Calibrated with stacking analyses on Planck
  - (Greco et al. 2015; Planck 2013 XI)
- Dominates even if CMB-S4 is used to remove contribution of known clusters
- Because clusters are hot ( $kT \sim \text{keV}$ ), the relativistic TSZ correction is detected in PIXIE
- PIXIE should be able to make  $> 100$  sigma detection of both mean  $y$  and characteristic temperature
- Sensitive to energy injection history





# Relativistic Correction

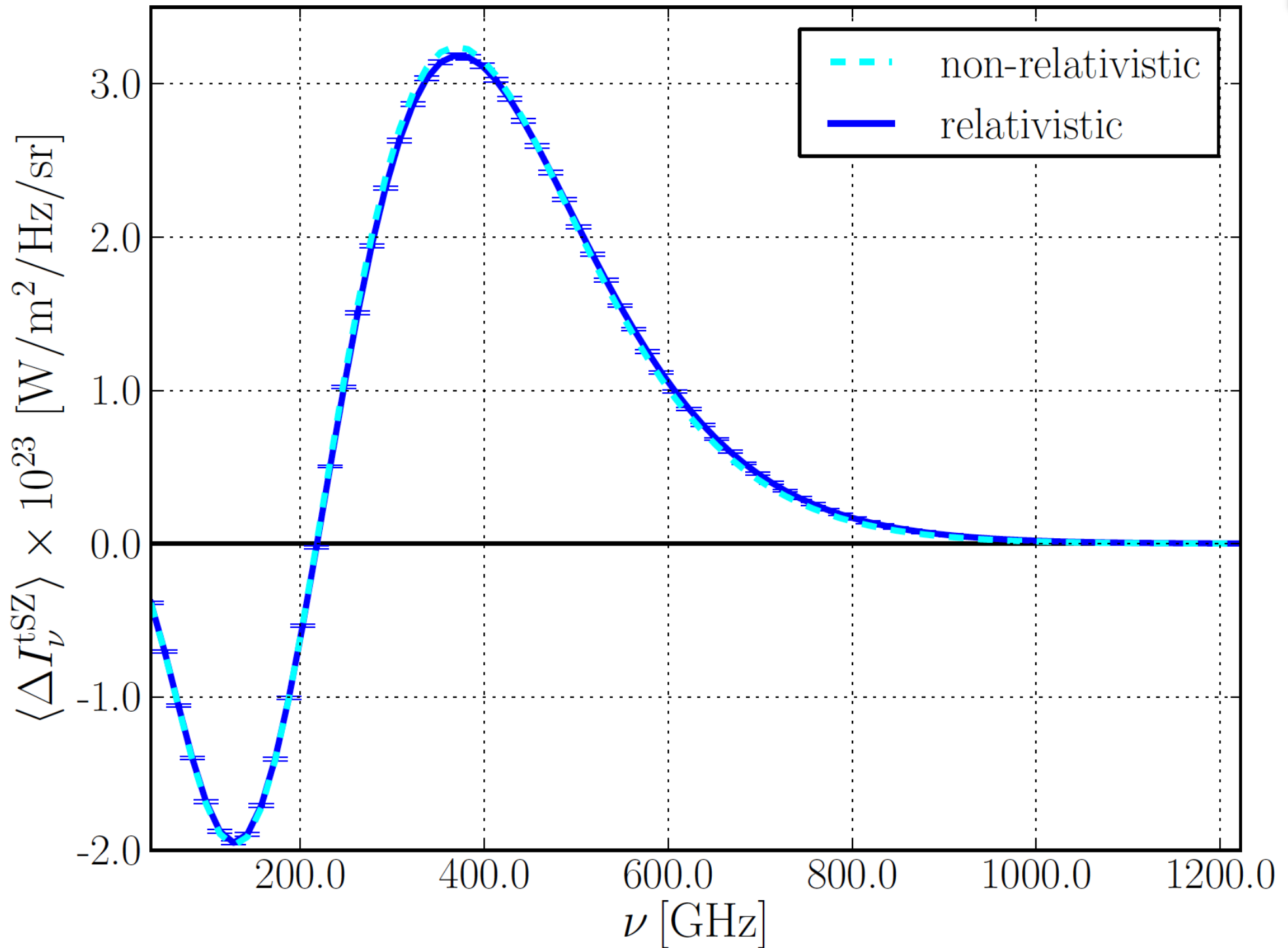
- Clusters are hot enough that the relativistic correction changes the shape of the spectrum



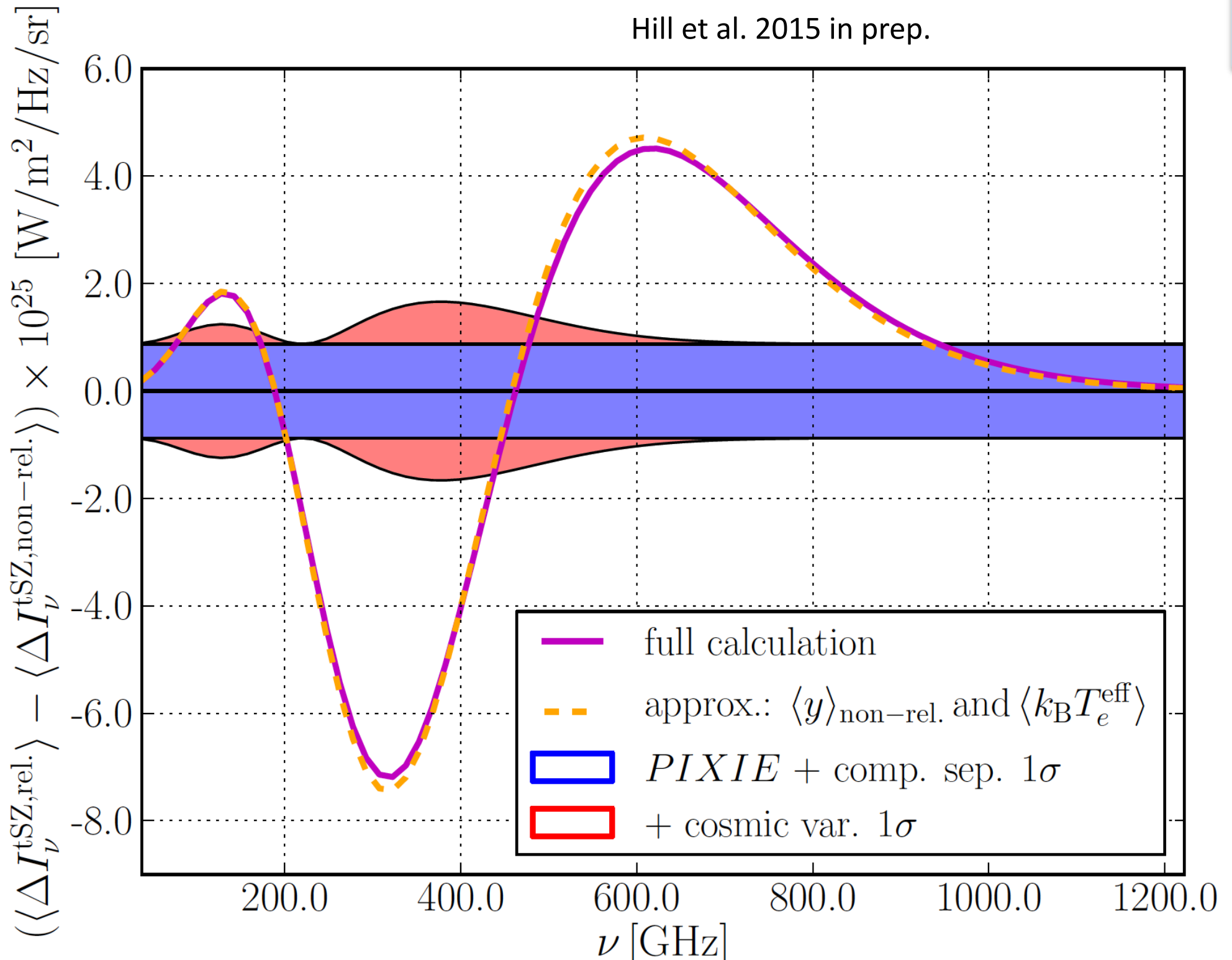
# Contribution to $\Upsilon$ from Clusters

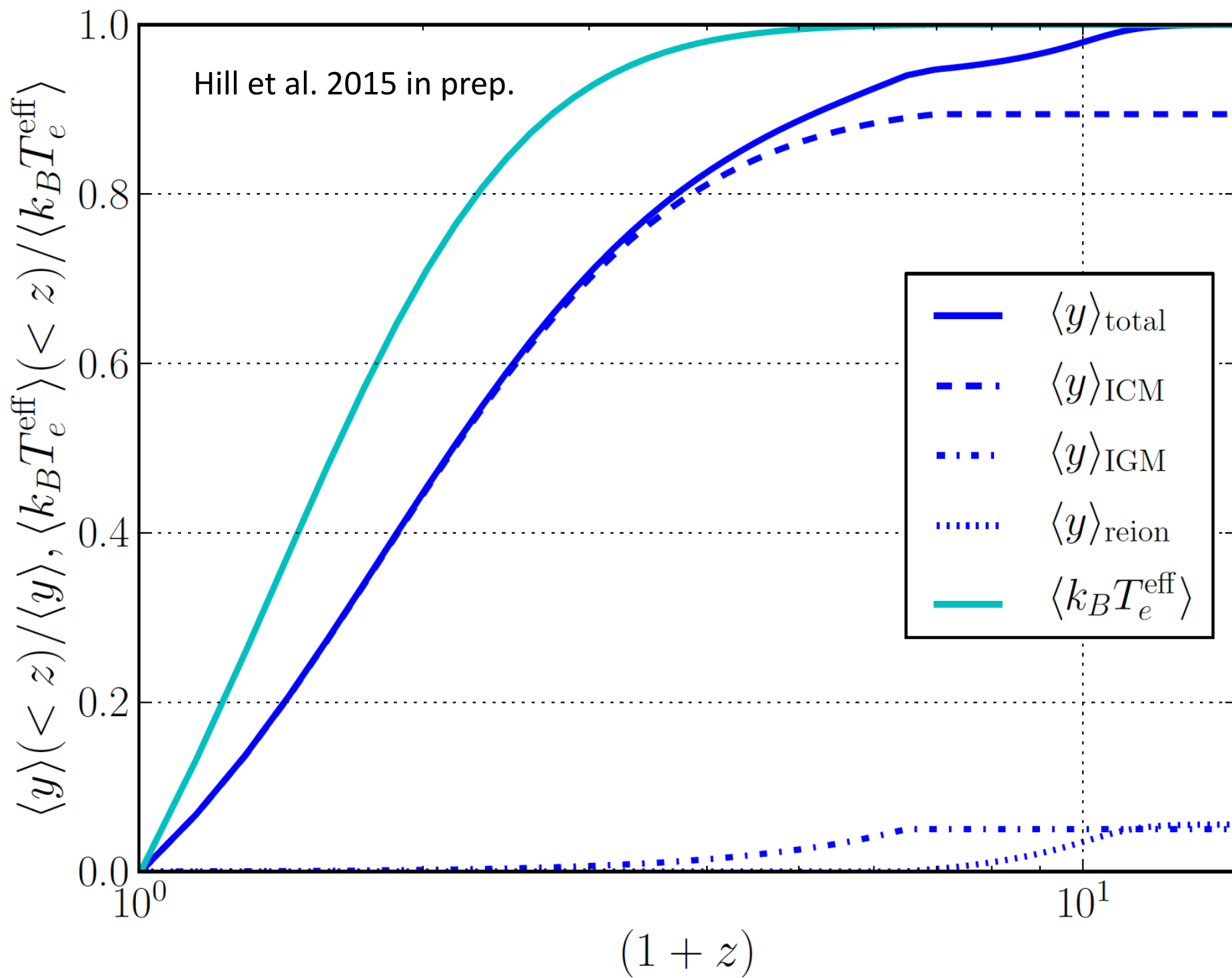
$$\langle \Delta I_\nu^{\text{tSZ}} \rangle = \int dz \frac{d^2 V}{dz d\Omega} \int dM \frac{dn}{dM} \int d^2 \hat{\mathbf{n}} \Delta I_\nu^{\text{tSZ}}(\hat{\mathbf{n}}, M, z), \quad (4)$$

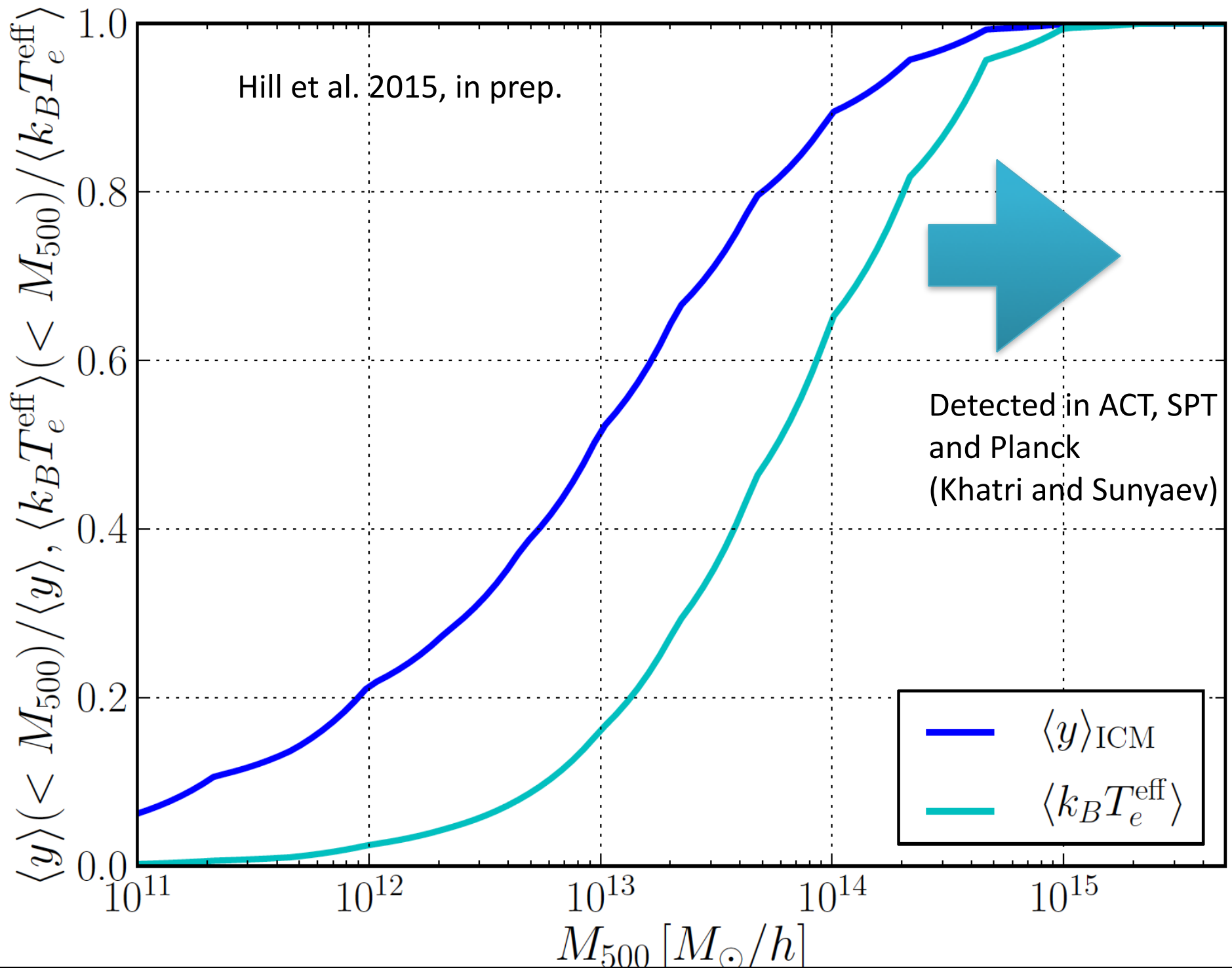
$$\langle k_B T_e^{\text{eff}} \rangle = \frac{1}{\langle y \rangle} \int dz \frac{d^2 V}{dz d\Omega} \int dM \frac{dn}{dM} \times \\ \int d^2 \hat{\mathbf{n}} k_B T_e(\hat{\mathbf{n}}, M, z) y(\hat{\mathbf{n}}, M, z),$$

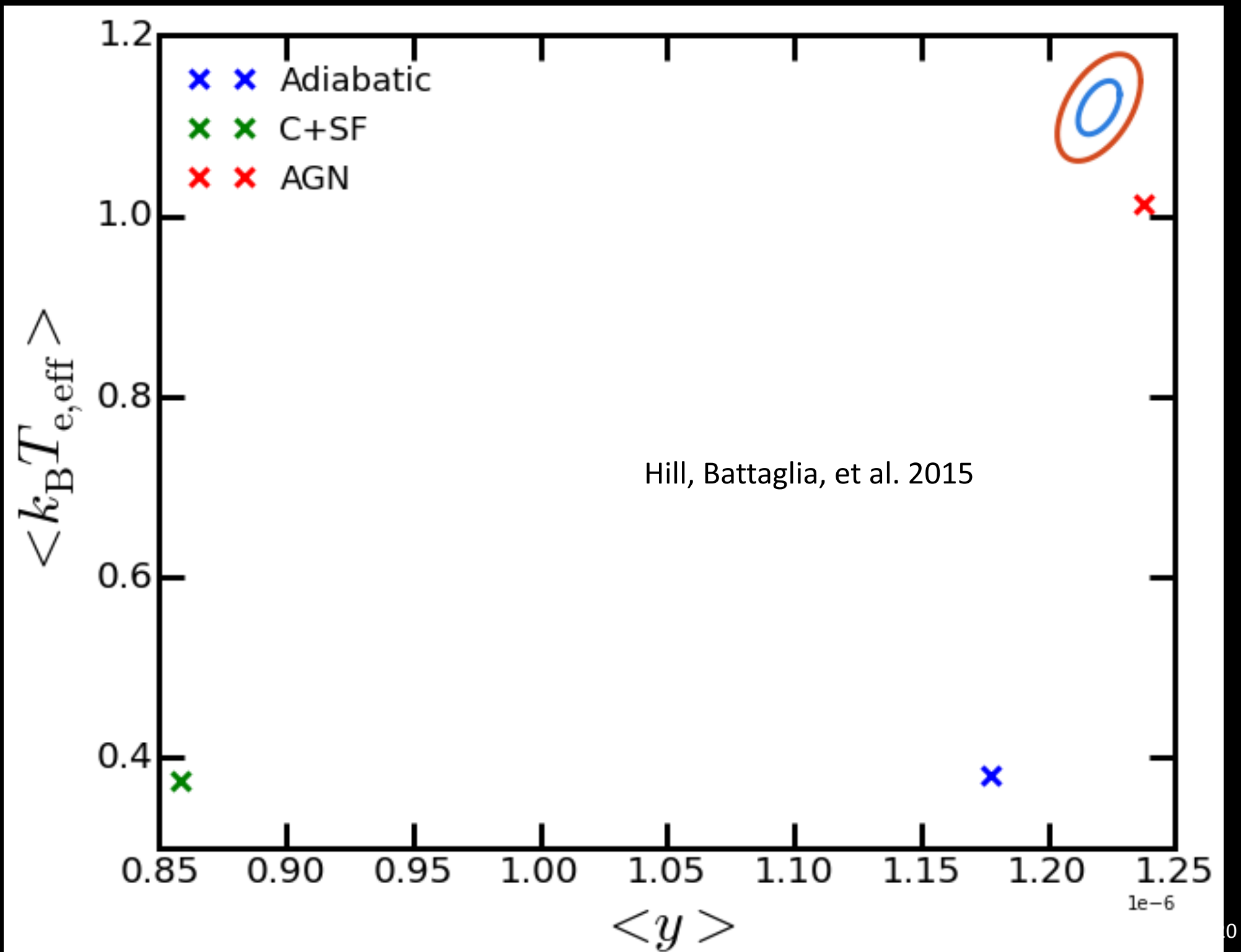




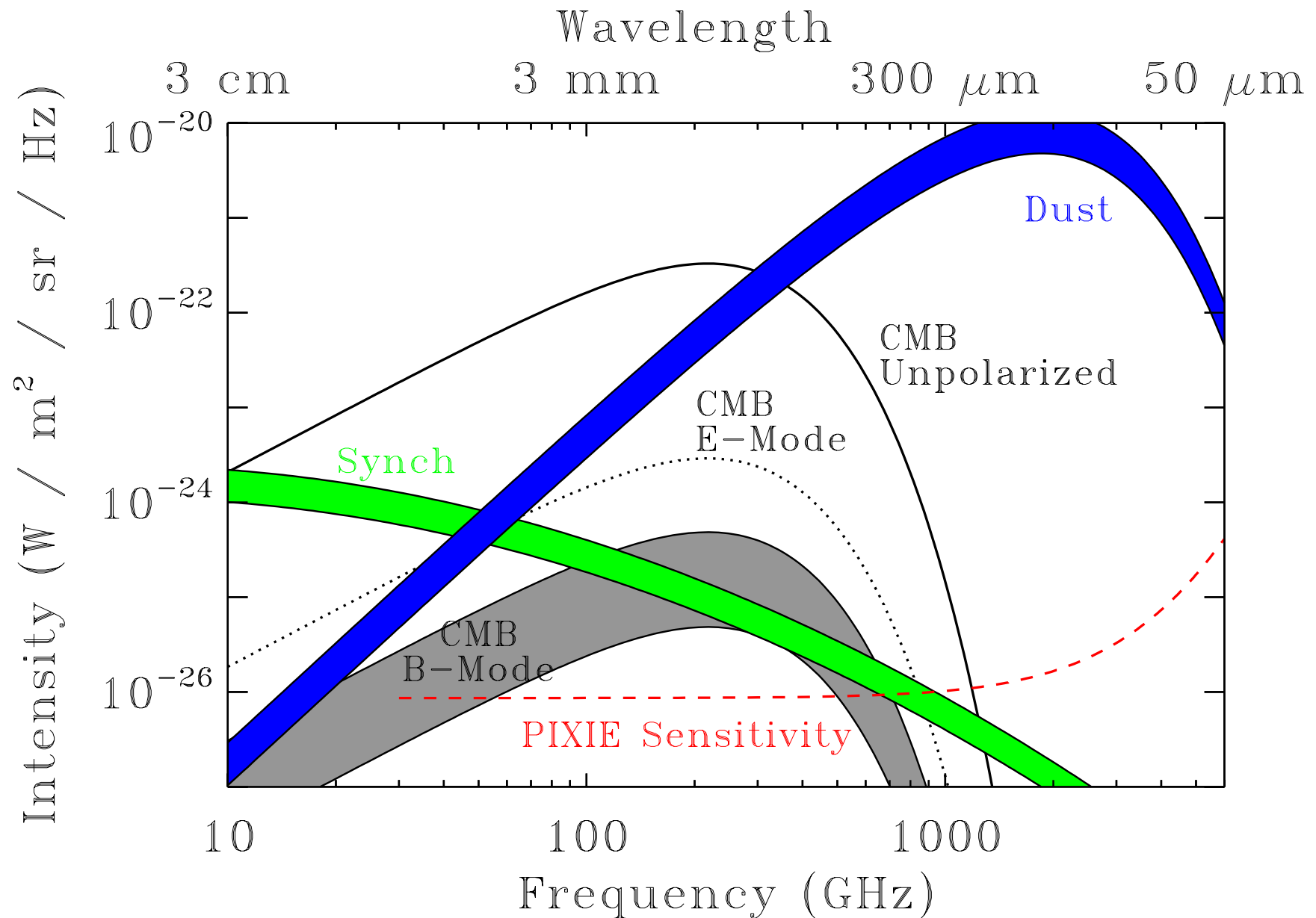








# Foregrounds scare me!

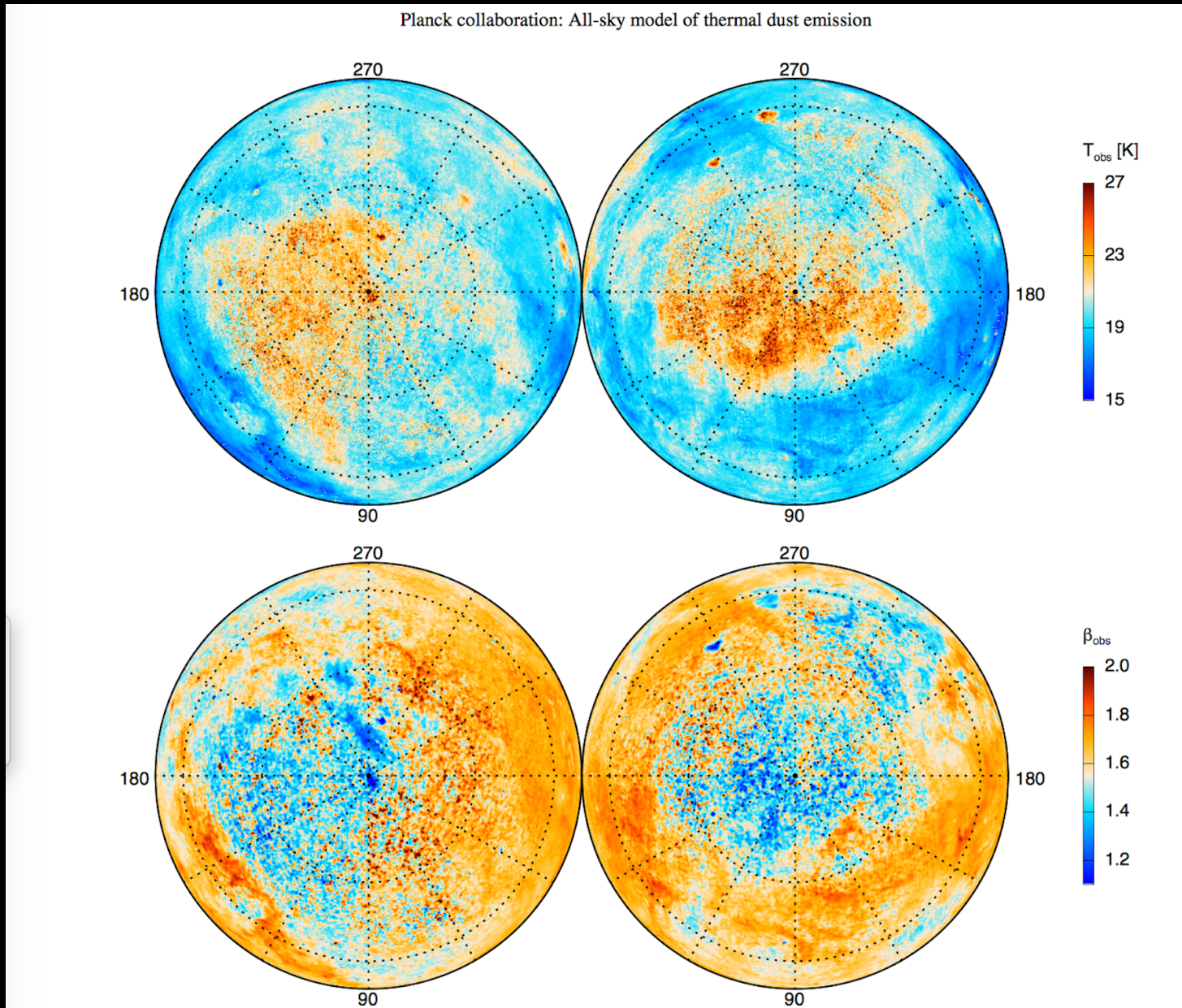


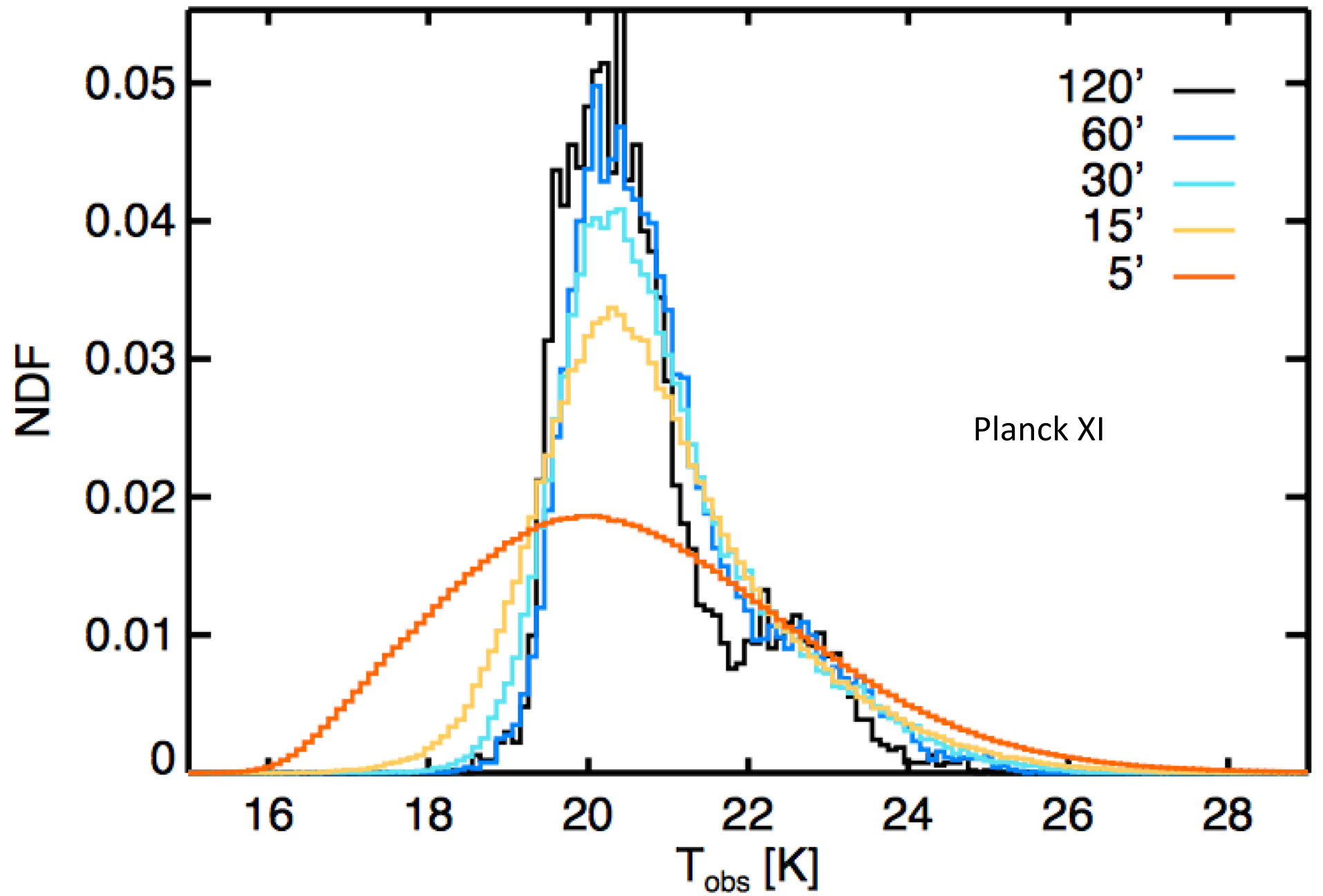
# Dust properties are varying

- Galactic dust temperature is slowly varying as a function of position
- Multiple temperatures along different lines of sight
- CIB amplitude and spectrum are also spatially varying
- Need to fit for  $\tau(T_{\text{dust}})$  at each position, possibly  $\tau(T_{\text{dust}}, \beta)$

$$I(\nu, \hat{n}) = \int dT_{\text{dust}} \tau(T_{\text{dust}}, \hat{n}) B_{\nu}(T_{\text{dust}})$$

# Planck dust temperature map

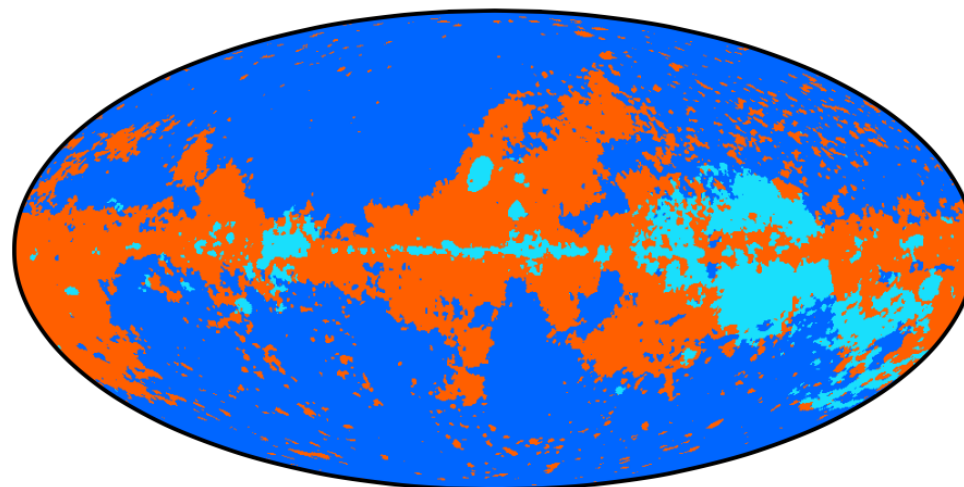




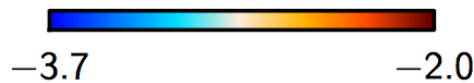
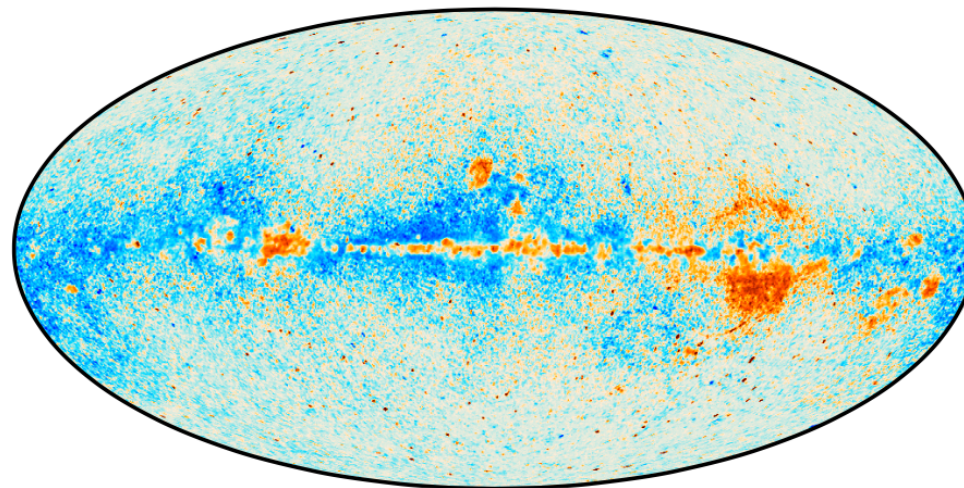


# Synch + Spinning Dust

Planck 2013 X



(a) Dominant low-frequency component map

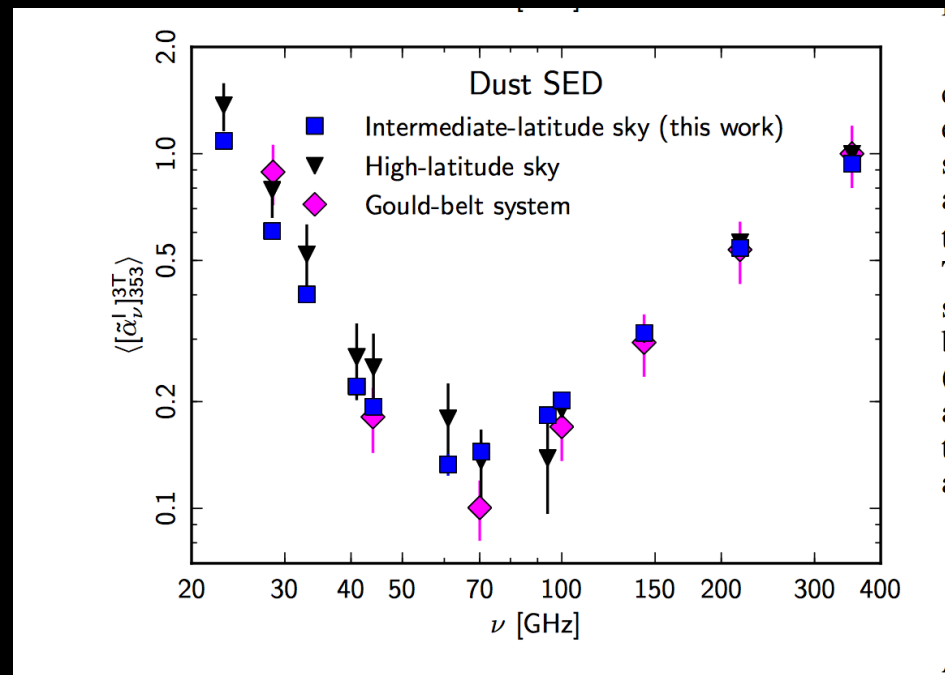


(b) Low-frequency component power-law index

**Fig. 23.** *Top:* dominant foreground component per pixel at 30 GHz in the FFP6 simulation. Dark blue indicates that synchrotron emission is the strongest component at 30 GHz, light blue indicates that free-free dominates, and orange indicates that spinning dust (AME) is the strongest component. *Bottom:* the recovered low-frequency power-law index derived from the same simulation.

# More worries

- Spatial variations in synch. spectral index
- Spatial variations in synch-dust cross-correlations
- Spinning dust, magnetized dust
- Spatial variations in extragalactic line emission
- Need more study!



Planck XXII

# Conclusions

- Photon spectrum records the energy input history of the universe since  $z \sim 2,000,000$
- $\mu$  distortions probe the power spectrum on scales far below CMB
- $z < 2$  groups and clusters will likely be the dominant source of  $y$  distortions
- PIXIE measurements of relativistic distortion should be very sensitive to energy input to clusters and baryon feedback
- Foregrounds are hard